Laboratory Test of Vibration of Micro/Nano Satellite for Environment Test Standardization

Laboratory Test of Vibration of Micro/Nano Satellite for Environment Test Standardization

By Amgalanbat Batsuren, Toru Hatamura, Hirokazu Masui and Mengu Cho

Kyushu Institute of Technology, Japan

This paper presents the basic research for establishing the qualification test (QT) level which the units have to pass to be sold as products for space usage. A laboratory test campaign has already begun for the study how the mechanical stresses distribute within the satellite body so as to define the unit QT level. In order to achieve that we carried out random vibration tests using a dummy satellite (50cmx50cmx50cm) and measured the distribution of acceleration inside the satellite. The research focuses on the provision of the physical basis of the test conditions to be defined in the new standard. We tried to identify the range of natural frequency and acceleration in the launching environment. The main parameters taken into consideration for analysis are the resonant frequencies and amplification of acceleration. The detailed test procedure, analysis method and primary results are herein reported.

Key Words: Vibration test, Acceleration, Natural frequency, PSD, Dummy Satellite

Nomenclature

AT	:	acceptance test
DM	:	dummy mass
OBC	:	on board computer
PAF	:	payload adapter
PCU	:	power control unit
PSD	:	power spectrum density
Q	:	Q factor
QT	:	qualification test
RF	:	radio frequency unit
U	:	standard deviation
U^2	:	sample variance
X_n	:	sample value
$\bar{X}$	:	average of sample

Subscripts

f	:	base frequency
f_0	:	resonant frequency
ȿ	:	damping rate
n	:	sample number
p	:	probability of lager value
k	:	frequency rate
t	:	transmittance

1. Introduction

As the use of micro/nano satellites proliferate all over the world, there is an increasing need of improving their reliability. As the reliability expected for micro/nano satellites are different from that of the large/medium satellites, however, the test level, duration and precision may not be same as those applied to testing of large/medium satellites. Prior to now there have been suitable environment test standards for large and medium sized satellites only which demands very high reliability. The existing standard is not suitable for micro/nano satellites that achieve low-cost and fast-delivery by using non-space qualified, Commercial–Off-the Shell (COTS) components extensively. There is a need of test standard to improve the reliability while keeping the nature of low-cost and fast-delivery. Currently there are conflicts of testing approach among developers and customers about how the environment tests should be implemented for micro/nano satellites and their units. Although the reliability expected for mirco/nano satellites are different from that of the large/medium spacecrafts, however, there are variations in the *test levels, durations* and *precisions* applied for the testings of the two types of satellites.

In 2011, Center for Nano-satellite Testing (CeNT), Kyushu Institute of Technology (KIT) initiated Nano-satellite Environment Test Standardization (NETS) project which is funded by Japanese government in order to develop environment test standardization for micro/nano satellites. The word "micro/nano-satellite" in this paper is used for satellites that are mostly made of COTS units, which typically has weight and size less than 50kg and (50cm x 50cm x50 cm) respectively. NETS project is an international collaborative effort to establish an international standard for testing of micro/nano satellites. The project goal is to further the growth of worldwide micro/nano satellite activities and utilization by proposing affordable and reliable tests to the community.

There are various environment tests to be dealt with in NETS projects. In the present study, we shall deal with vibration test. At present, a large level of acceleration is applied to satellite units during the test, which has been derived by taking into account various safety margins. The bases of the margins are not always clear.

At the same time, there are many COTS-based units claimed to be good for micro/nano satellite usage in the market. Those products often however lack of test history under which they are qualified for the space use. Satellite developers are caught in the middle whether they choose expensive and long-delivery product weighing more emphasis on the reliability or choose the COTS-based product taking the risk of having a product that may not satisfy their criteria. If the COTS-based product passed a certain level of testing defined in a standard, the satellite developer may choose the COTS-based units with more confidence. Currently there is no such standard for micro/nano satellite units. One of purposes of NETS project is to define the qualification test (QT) level which the units have to pass to be sold as products for space use.

For the unit QT, the standard NETS project aims will provide the minimum guarantee that a given unit sold as "a satellite unit" has a certain level of tolerance against space environment. Therefore, the unit QT in the standard does not include proper margin against the maximum predicted environment stress, which depends on each satellite. The satellite developers who procure the unit may carry out another QT using a dedicated test model. They may carry out PFT using a flight model or only AT taking the risk of little margin. The satellite developer shall provide the test levels and duration of the additional QT, AT or PFT.

Random vibration tests were conducted using different acceleration ranges from 0.3Grms to 9.0Grms with frequencies in the range of 20 to 2000Hz. The vibration signal corresponding with the particular direction was applied for 50 s. We attached accelerometers inside the satellite and studied the distribution of mechanical stress. In total, 15 cases were studied. We investigated the resonance frequency, resonance frequency ratio and amplification factor of each tested positions of dummy satellite. The amplification factor is defined as the square root of the ratio of the measured PSD value at a given point by the base level as shown in the Eq. (1) below:

$$AF = \left(\frac{PSD_{\mathrm{m}}}{PSD_b}\right)^{\frac{1}{2}} \qquad (1.)$$

where AF is the Amplification factor, PSD_m is the measured PSD value, and PSD of base level is referred as PSD_b.

From the tested data, we calculated the resonance frequencies and max amplification factor in the X,Y and Z vibration axis. After series of vibration tests we have investigated that there are several vibration modes for the satellite due to satellite structure and panels. In the present study, we deal with only local vibration mode which is in the frequency range, 300-2000Hz. We estimated the range of resonance frequency and the amplification ratio with the data results of the 50cm, 50kg dummy satellite random vibration test for 9Grms test level. We obtained interval estimation of population mean of resonance frequency and the amplification ratio in the local vibration mode.

The paper is composed of four parts. The second part describes the experiment. The third part describes the results and their analysis and in the last the part overall experiment was summarized.

2. Experiment

The experiment was conducted on a vibration table at CeNT, KIT. A dummy satellite of 50cmx50cmx50cm as shown in Fig. 1 was tested extensively in this experiment. The internal structure of the satellite body is made of four panels with two third the width of the satellite body cross linked forming a "Yojo-han (four half tatami)" when viewed from the top, it can be seen as the popular layout of tatamis, Japanese traditional carpet. There is a square column made by the four panels at the center. The internal and external panels are made of Aluminum (alloy:5052). The dummy satellite is a copy of 50kg-50cm nano-satellite that was previously developed for remote sensing purpose as illustrated in Fig.1.

The advantage of the Yojo-han satellite is its easiness to install and components' accessibility. Because the structural style is composed of four internal panels and five external panels fixed to each with bolts, however, it may cause more mechanical stress than other structural styles such us center cylinder and panels. This design is made to provide large enough area for mounting the units and components while being sturdy. All the units and subsystems are mounted within the cuboid except sensors and antennas that are mounted outside.

The dummy satellite was made of basic satellite functions such as RF transmitter, PCU, battery and computer. Although the other units are made by dummy mass with heater inside, the units mentioned above and the satellite structure are of flight quality. Accelerometers were attached at the positions of internal and external panels(i.e near the units) and jig which is used. The dummy satellite was fixed to the vibration machine using a mock-up of payload adaptor fitting (PAF) and a jig as shown in Fig.2.

Vibration tests were conducted to gather distribution of the amplification factor and the resonance frequency to obtain the statistics of those among different acceleration ranges from 0.3Grms towards 9Grms random vibration (20-2000Hz).

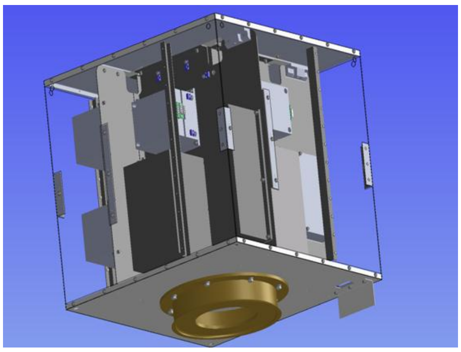

Fig. 1. Structure of the dummy satellite bus.

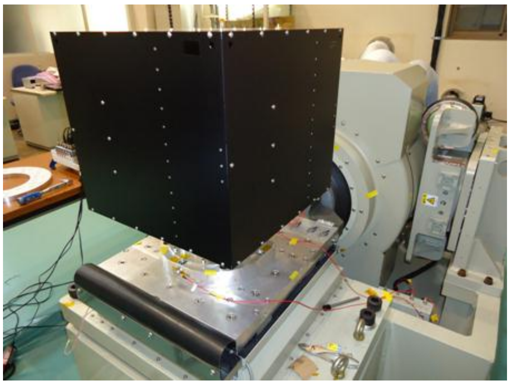

Fig. 2. Dummy-satellite on the Vibration Machine.

In total, we measured at 46 points. 4 points (three monoaxial accelerometers fixed at the same point to measure for 3 axis) are on the top corner, 3 points are on each external panel where one axis accelerometers were attached, and we measured 18 points at dummy masses/units that are placed in internal panels. Fig.3 shows the all accelerometer locations of on the dummy satellite for this experiment.

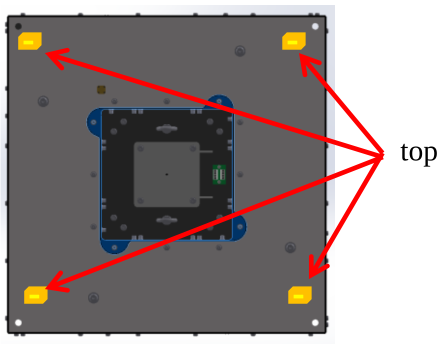

a). Top view

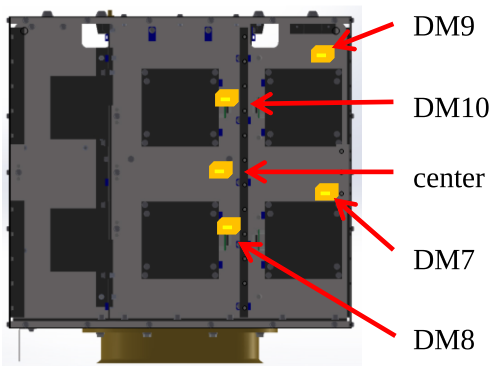

b). -Y internal panel view

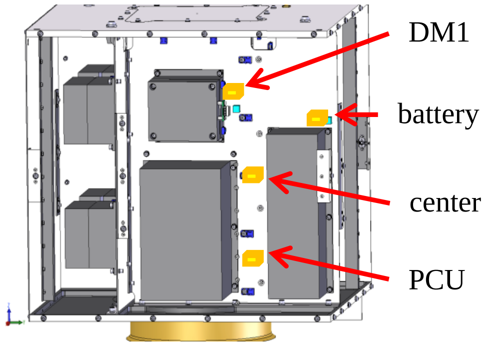

d).+X internal panel view

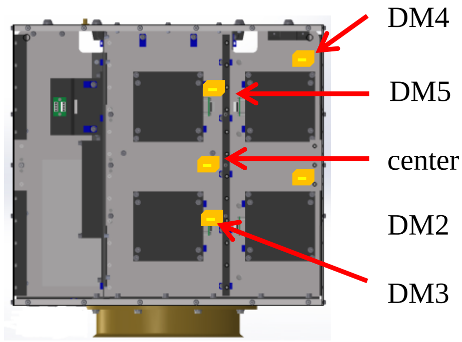

e). -X internal panel view

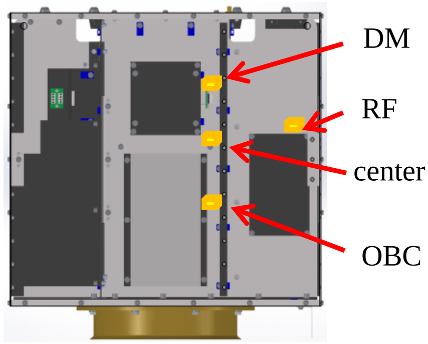

f). +Y internal panel view

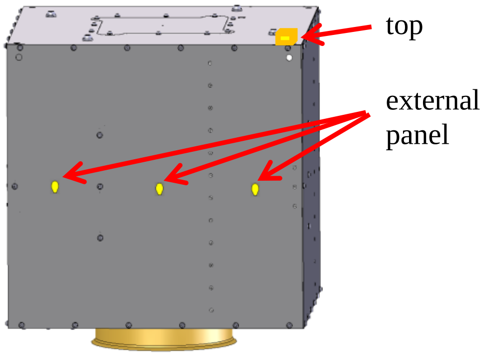

g). External panel view

Fig. 3. Overview of the units and accelerometer positions.

As shown In Fig 4, the accelerometer was placed near the dummy mass/ units. They are placed on the internal panel of the satellite rather than the box of the units or dummy mass because the acceleration used for reference in the unit vibration test were the ones of the base plate, i.e. the satellite internal panel.

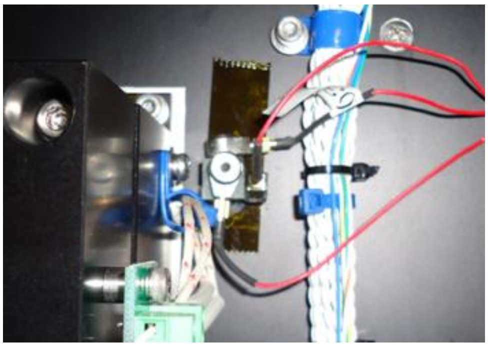

Fig. 4. Photo of mounted accelerometers

The locations of the sensors are listed in Table 1.

Table 1. The accelerometers' locations

Sensor position	Location	Sensor axial direction	Sensor model
DM4	-x internal panel	x,y,z	EMIC 710-C
DM2	-x internal panel	x,y,z	EMIC 710-C
DM5	-x internal panel	x,y,z	EMIC 710-C
Center	-x internal panel	x,y,z	EMIC:710-C
Top	-x,–y corner	x,y,z	EMIC:710-B3
ext. panel	-x external panel	x,x,x	Endevco.2222C
DM3	-x external panel	x,y,z	EMIC 710-C
DM1	+x internal panel	x,y,z	EMIC 710-C
PCU	+x internal panel	x,y,z	EMIC 710-C
Battery	+x internal panel	x,y,z	EMIC 710-C
Center	+x internal panel	x,y,z	EMIC 710-C
Top	+x,+y corner	x,y,z	EMIC:710-B3
ext. panel	+x external panel	x,x,x	Endevco.2222C
DM6	+y internal panel	x,y,z	EMIC 710-C
OBC	+y internal panel	x,y,z	EMIC 710-C
RF	+y internal panel	x,y,z	EMIC 710-C
Center	+y internal panel	x,y,z	EMIC 710-C
Top	+y,-x corner	x,y,z	EMIC:710-B3
ext. panel	+y external panel	y,y,y	Endevco.2222C
DM7	-y internal panel	x,y,z	EMIC 710-C
DM8	-y internal panel	x,y,z	EMIC 710-C
DM9	-y internal panel	x,y,z	EMIC 710-C
DM10	-y internal panel	x,y,z	EMIC 710-C
center	-y external panel	y,y,y	EMIC 710-C
top	-y,+x corner	x,y,z	EMIC:710-B3
jig		x	EMIC 735
jig		z	EMIC 735

Only one-axis accelerometers were used in the test. The accelerometers were attached to the internal and external panel in the direction of X, Y and Z axis as shown in Fig. (4). Each accelerometer (manufacturer: EMIC Corp., model: 710-C, 710-B3, 735 and Endevco. 2222C) was connected to a charge amplifier (manufacturer: SHOWA SOKKI Corp., model: Showa 4035). The data was taken through DAQ (manufacturer: National Instruments, model: NI CDAQ-9178) to a PC with USB cable. The maximum of 24 channels of the analog signal with the range of ±10V from the charge amplifier was taken simultaneously and converted to digital signal at 16 bit DAQ (5000 samples) for 50 seconds and the Fast Fourier Transform (FFT) was applied by a standard desktop PC using Labview.

In the test, the vibration level was controlled by monitoring the two monoaxial accelerometers(control accelerometer) attached rigidly on the jig aligned with the axis of applied vibration to check the input signal and taking the average of them. Base accelerometers (ch23, ch24) for calculating amplification ratio were mounted besides the control accelerometers as illustrated in Fig 5 below.

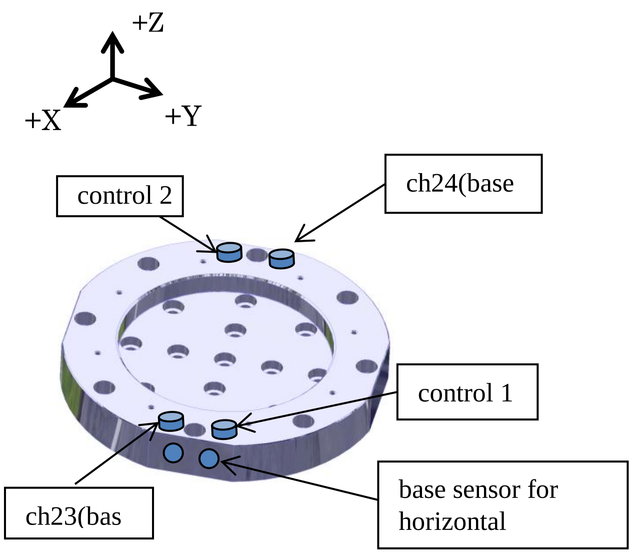

Fig. 5. Mounting position of base and control accelerometers on the jig.

Vibration tests were performed along the X, Y and Z satellite axes. Testing along the Z axis (longitudinal vibration test) was performed mounting the satellite on the shaker using the jig shown in Fig.5. The same shaker and support, connected to the horizontal vibration table, were used for the X and Y axes vibration test (transverse vibration).

The base acceleration level of the vibration testing machine is listed in Table 2. The shape of input level comes from the Space and Missile Systems Center Standard (SMC). Using the same shape as shown in Fig.6, the level was shifted so that we could test 5 levels, 0.3Grms, 1Grms, 3Grms, 6Grms and 9Grms. The test started from 0.3Grms toward 1.0Grms and 9.0Grms at the end. Each vibration was applied for 50 seconds.

When we performed the random vibration analysis, an input spec was given in a form such as the log-log plot in the figure or written in the table as shown in Table 2 and Fig.6 below.

Table 2. Random vibration spectrum curve values of 9.0Grms.

Frequency (Hz)	Amplitude
20	0.01 g^2/Hz
20 to 100	+3dB per octave slope
100 to 1000	0.06 g^2/Hz
1000 to 2000	-6dB per octave slope
2000	0.01 g^2/Hz

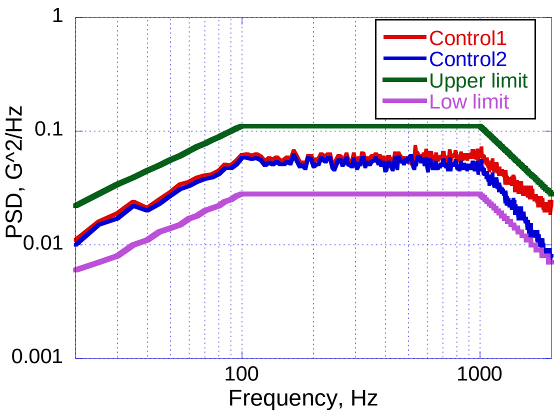

Fig. 6. Vibration profile with RMS of 9Grms

After each vibration, we checked the characteristic changes by performing low level random, i.e. 0.3Grms to check if there are no changes for natural frequency etc.

3. Test results and data analyzing

As mentioned earlier, we used random vibration input level for the experiment. Because as opposed to periodic signals, random vibration has continuous spectra, that can contain all frequencies. We used result of PSD for the following derivation of the test result. The PSD of random vibration signal contains all frequencies in the particular frequency band. There is a wide range of methods available for solving forced response simulation. In case we calculate steady-state solution, the simplest way was to use the Fast Fourier transform (FFT) to solve the solution in the frequency domain.

The plotted data of PSD (Power Spectrum Density) of z axis sensor on the position of DM1, PCU and Battery for 0.3Grms and 9Grms levels of vibration in z-direction are shown in Fig 7 and Fig 8. The figures show the PSD value measured from accelerometers to measure z axial acceleration attached to DM1, PCU and Battery that are placed at +x internal panel for the 0.3Grms and 9Grms input level(axial direction). The figures show that there is no significant difference of the resonance frequencies in each vibration level.

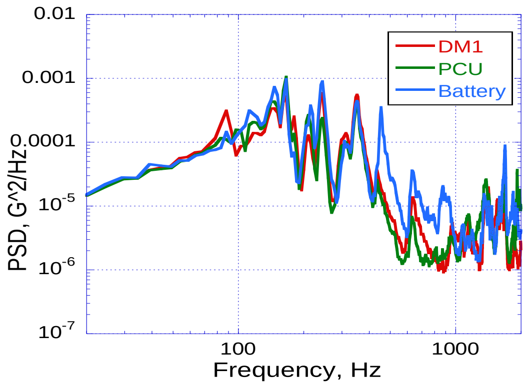

Fig. 7. PSD value (0.3Grms,z-axis sensor and z-axial direction vibration).

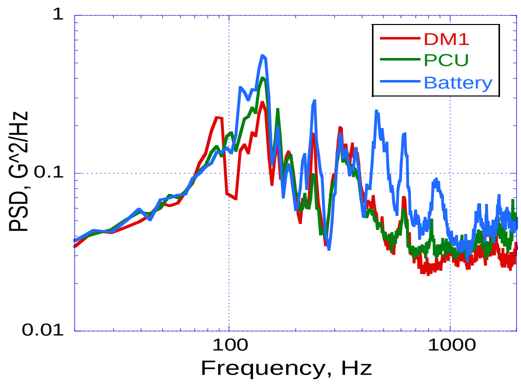

Fig. 8. PSD value (9Grms,axial direction vibration)

The amplification factor was calculated from PSD of measurement point divided by base level and square rooted as mentioned earlier. Peak amplification factors were derived among the amplification factors corresponding to resonant frequency of each channel of measurement. Fig. 9 shows the maximum of the peak amplification factor at the various test level from 0.3Grms to 9Grms. Here, the maximums of peak amplification factors means the maximum value of the peak amplification factors measured from all points and the minimums of peak amplification factors were derived from all minimum value of peak amplification factors of all measured points. In this test, the maximum of the peak amplification factors were 42, 32, 24, 21, 18 for 0.3Grms, 1Grms, 3Grms, 6Grms and 9Grms respectively as plotted in Fig.10 below. The figure shows that peaks of amplification factor decreased with increased input acceleration level.

The peak amplification factor decreases as the base vibration level increases. From Fig.7 and 8, we can see that the peaks become smooth at higher G. It is because the vibration transmittance is not really a simple linear process. Non-linear effects smoothen the peak as the vibration force increases. Because our concern is whether units or a satellite can survive the harsh environment, we use the experimental results obtained from the high level acceleration to derive the unit test level. By using the result of the high level acceleration, the peak values in PSD are reasonably smoothed out and lead to a less severe test level.

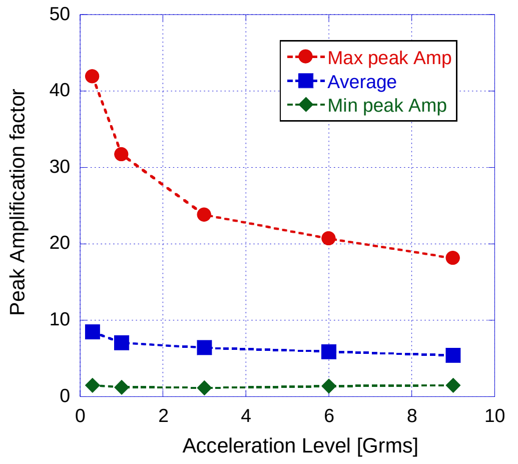

Fig. 9. Peak amplitude ratio comparison

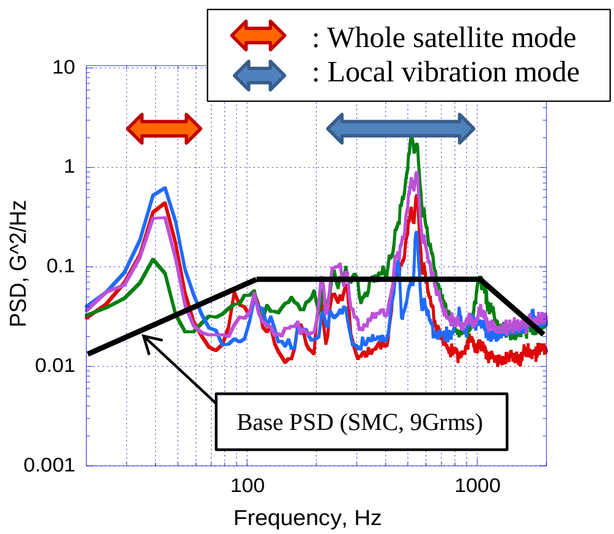

Fig. 10. Vibration response at internal panel
(Vibration is in the direction perpendicular to the axial direction)

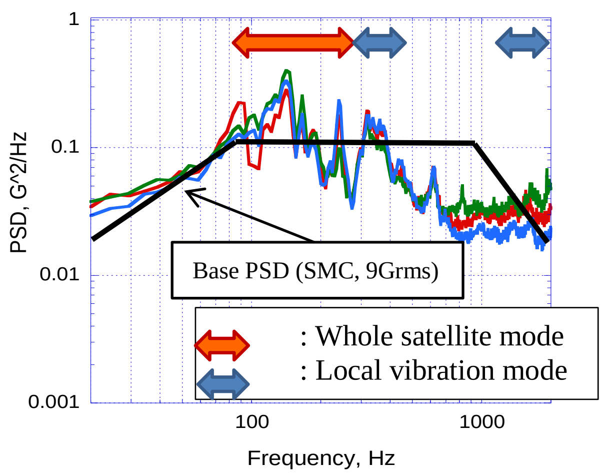

Fig.11. Vibration response at internal panel(Vibration is in axial direction)

Figure 10 and Figure 11 show the example of PSD waveform measured at 9Grms when the base vibration is given in the direction perpendicular to the axis and in the direction parallel to the axis. We notices several features. Peaks at low frequencies typically less than 300Hz. Those peaks are originated from the resonance of entire satellite structures to the vibration. We call them "*Whole satellite mode*". In Ref.(2) , we analyzed the whole satellite mode of various 50cm-class micro satellites. The resonances appear between 30 and 70Hz for the vibration perpendicular to the thrust axis and 100 to 200Hz for the vibration parallel to the thrust axis(axial direction).

The peaks at frequencies higher than 300Hz (although the value 300Hz is rather arbitrary) are originated from the resonance of satellite internal structure. They depend on various factors, such as how the internal structure is arranged, direction/thickness/material of the internal panel, the sensor location, etc. We call those peaks "*Local vibration mode*". Internal units are exposed to those modes inside a satellite. To establish the standard test level, we need to investigate the ranges of the whole satellite mode and local vibration mode in terms of the amplification factor at the peak and the resonant frequencies. Ref.(2) deals with the range of the whole satellite mode. In the present paper we focus on the local vibration mode, 300 to 2000Hz. We will investigate the range based on the statistical analysis similar to Ref.(2).

When we calculate the range of the amplification factor, the resolution of PSD becomes important. First we calculated and plotted PSD using 0.6Hz of frequency step, the PSD was very high and sharp. If we take the statistics to find the interval of the peak value, we would have seen extremely high level of acceleration, which is rather unrealistic. Unless the natural frequencies of the satellite internal panel and the unit structure matches exactly, it is very unlikely the units will be accelerated at the high PSD value. The important to thing is to give the energy contained within a certain bandwidth centered around the natural frequency.

Therefore, we changed frequency increment and *frequency resolution* which is the distance between two frequency values in the Discrete Fourier Transform (DFT) from Δf=0.6Hz to Δf=4.8Hz (1/3 octaves) to ensure smoother PSD. After changing frequency resolution to 4.8Hz, PSD becomes smoother than previous resolution. In order to check if we can use this frequency resolution for our further analyzing, we compared RMS's of PSD for several frequency resolutions as listed in Table 3. As shown in the Table, we found that there was no RMS differences in each frequency resolution even PSD level is increased with reducing frequency resolution. Therefore, we can give the energy properly to a unit even if we use the test level derived from the low resolution.

Table 3. RMS of PSD comparison in different frequency resolution

ch	Δf=0.6	Δf=1.2	Δf=2.4	Δf=4.8
1	9.64	9.64	9.64	9.64
2	16.60	16.60	16.60	16.60
3	9.18	9.18	9.19	9.19
4	11.30	11.30	11.30	11.30
5	23.30	23.30	23.30	23.30
6	10.00	10.00	10.00	10.00

In this paper, we only deal with those local vibration modes. Therefore we gathered data in the frequency range 300 to 2000Hz. We classified local vibration mode(300-2000Hz) into 2 groups: 300-1000Hz and 1000Hz-2000Hz. Because we noticed from the PSD waveform that in most cases there are several resonance frequencies from 300Hz to 2000Hz as seen in Fig.10 and Fig.11. Then we generated all sensors' PSD in these two local vibration modes group separately using 4.8Hz frequency resolution. We found peak PSD of resonant frequencies of all channels in each group. In order to find resonant frequencies, we gathered PSD data of same axis accelerometer with vibration direction. In particular, we analyzed PSD data of x,y,z axis accelerometers' in the x,y,z vibration direction respectively. From the mechanical point of view, although the momentum can generate perpendicular force to the vibration direction, but this force is lower than that of the vibrating direction and is dependent on the satellite structure. Here x and y vibration direction represents perpendicular to the axial direction(horizontal acceleration) and z vibration direction represents the axial direction(vertical acceleration) herein.

We do the statistical analysis to derive the upper and lower limit of the average values of the amplification factor and the resonant frequency. We use a method of t-distribution function. We required a distribution that will enable us to compute confidence limit for true mean μ, knowing sample variance *U* but not true varianceσ. In this reason, *t*-distribution statistical method was identified and taken into consideration. The *t* distribution is a symmetric distribution that resembles the normal distribution can be shown to be associated with the distribution of sample means.

The range of the population mean was described with the average of samples $\bar{X}$, sample number *n*, probability of a larger value *p* and sample variance *U*. $\bar{X}$ is the sample mean represents the average value of tested data. X_L is the lower limit of estimated value, and X_U is the upper limit of estimated value.

In seeking a sample estimator of σ, it is natural to start with the deviations $x_i = X_i - \bar{X}$ of the sample observations from the sample mean. Ref(3). In statistical analyzing the most widely used estimator of σ is the sample standard deviation, denoted by *U* here. The formula defining *U* is shown in Eq. (2).

$$U = \sqrt{\sum_{i=1}^{n} (X_i - \bar{X})^2 / (n-1)} \quad (2.)$$

$$X_L = \bar{X} - p * \frac{U}{\sqrt{n}} \quad (3.)$$

$$X_U = \bar{X} + p * \frac{U}{\sqrt{n}} \quad (4.)$$

We gathered the peak amplification factors and resonance the frequencies related at each peak amplitude ratio measured at 18 points located inside the dummy satellite . We use n=18 and $p(t_{0.05})$=2.11 to calculate X_L and X_U as shown in Eq. (3) and Eq. (4). Reliability coefficient was chosen as 95%.

The interval of the population mean of the resonance frequency in the frequency range 300-1000Hz and 1000-2000Hz are listed in Table 4 and Table 6 respectively. The interval of the amplification factor are listed in Table 5 and 7, respectively. .

Table 4 . Population mean of resonance frequency(300-1000Hz)

	Resonant frequency[Hz]		
	Perpendicular to the axial(x)	Perpendicular to the axial(y)	Axial direction (z)
$\bar{X}$ (Sample mean)	566	586	320
U (Sample standard deviation)	281	760	179
X_L Lower value	426	208	231
X_U Upper value	706	964	409

Table 5 . Population mean of amplification factor (300-1000Hz)

	Amplification factor		
	Perpendicular to the axial(x)	Perpendicular to the axial(y)	Axial direction (z)
$\bar{X}$(Sample mean)	2.7	3.7	1.4
U (Sample standard deviation)	1.1	2.4	0.3
X_L Lower value	2.1	2.5	1.3
X_U Upper value	3.3	4.9	1.6

Table 6 . Population mean of Resonant frequency (1000-2000Hz)

	Resonant frequency[Hz]		
	Perpendicular to the axial(x)	Perpendicular to the axial(y)	Axial direction
$\bar{X}$ (Sample mean)	1798	1798	1694
U (Sample standard deviation)	865	1746	601
X_L Lower value	1368	930	1395
X_U Upper value	2228	2667	1993

Table 7 . Population mean of amplification factor (1000-2000Hz)

	Amplification factor		
	Perpendicular to the axial(x)	Perpendicular to the axial(y)	Axial direction (z)
$\bar{X}$ (Sample mean)	2.3	2.3	2.0
U (Sample standard deviation)	3.8	3.6	2.5
X_L Lower value	0.4	0.4	0.7
X_U Upper value	4.1	4.1	3.2

Then, we also calculated the vibration transmittance outside of resonance frequency range. We calculated the vibration transmittance apart from the resonance frequency range. Transmittance τ is described with damping rate ζ and frequency rate κas shown in Eq. (5) and Fig.12. We approximate the vibration by a single-degree-of-freedom vibration system. In addition, frequency rate κ is described with excited frequency of the base f and resonance frequency f_0 as shown in Eq. (6).

Damping rate ζ has the relation with Q factor as shown in Eq. (7). The quantity Q is a measure of the sharpness of resonance of a resonant vibratory system having a single degree of freedom. In a mechanical system, this quantity is equal to one-half the reciprocal of the damping ratio as shown in Eq. (7). It is commonly used only with reference to a lightly damped system and is then approximately equal to Transmittance or Transmissibility at resonance. Transmissibility is the ratio of the response amplitude of a system in steady-state forced vibration to the excitation amplitude. In our case, transmittance is equal to the amplification factor.

$$\tau = \sqrt{\frac{1+(2\zeta\kappa)^2}{(1-\kappa^2)^2+(2\zeta\kappa)^2}} \quad (5.)$$

$$\kappa = \frac{f}{f_0} \quad (6.)$$

$$Q \approx \frac{1}{2\zeta} \quad (7.)$$

Vibration transmittance at the outside (964Hz-1368Hz) of resonance frequency was calculated with resonance frequency f_0 and Q factor at boundary conditions. We used Eq.(5) for calculating the gradient value of transmittance from 964 Hz to 1368Hz. We assumedζ=0.1.

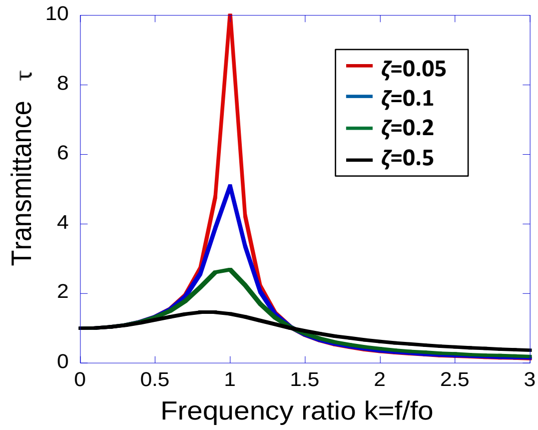

Fig. 12. Transmittance (τ) against frequency ratio (κ)

We now propose the unit QT test level with the values listed in Table4 to Table7.

Total of six (6) cases were studied based on the local vibration mode using three (3) axes of the vibration direction namely; perpendicular to the axial direction(x), perpendicular to the axial direction(y) and axial direction (z) in particular for frequency ranges of 300-1000Hz and also for 1000-2000Hz. For the resonance frequency, we chose the widest frequency range case for further estimation. The widest frequency interval is between 208Hz and 964Hz in the frequency range of 300-1000Hz as shown in Table 4. On the other hand, this interval accommodates the upper and lower frequencies of the other two, (426,706Hz) and (231,409Hz) which are within the range of 208-964Hz. In the selected frequency range the amplification factor of 2.5 was finally deduced as the unit QT test level in the local vibration mode.

We chose 2.5 because the test level we are trying to propose is to guarantee the minimum level of assurance. Unit manufacturers have no way of knowing in which direction their products will be mounted in the satellite. It could be on the plane perpendicular to the thrust axis or on the plane parallel to the thrust axis. If we chose 1.3 as the amplification factor, we can not know whether a product that passed the vibration test with 1.3 amplification can pass if it is shaken with 2.5 amplification in the perpendicular direction to the thrust axis. At least it is possible that the product will undergo vibration amplified by a factor of 2.5 in one direction.

After determining the amplification factor for 300-1000Hz we now determined amplification factor and resonance frequency range for 1000-2000Hz interval. From the estimated values in tables 6 and 7 the amplification factors were 0.4, 0.4 and 0.7 for directions perpendicular to the axial (x), (y) and axial (z) respectively. With the effect of damping due to structural fixations of the dummy satellite we have amplification to be less than 1. We can choose 0.7 as the amplification factor for the standard if we use the same logic for 300 to 1000Hz. Instead we select 1, no amplification, for the sake of simplicity.

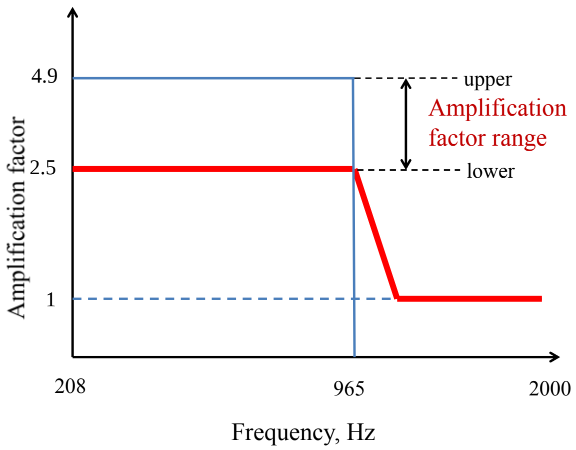

Fig.13. The amplification factor and resonance frequency range for unit QT test level

Fig. 14 below shows the AT level of random vibration for various rockets in the frequency range of 300-2000Hz. In this research, for determining the unit QT level, we adopted the SMC shape as indicated in the red colored curve(Level A) which has an RMS level of 6.7 as shown in Fig.14. Level B which stands for AT test level with of a rocket an RMS level of 7.3Grms while Level C stands for the AT test level of another rocket with an RMS level of 4.6Grms. These RMS values are calculated between 300 to 2000Hz.

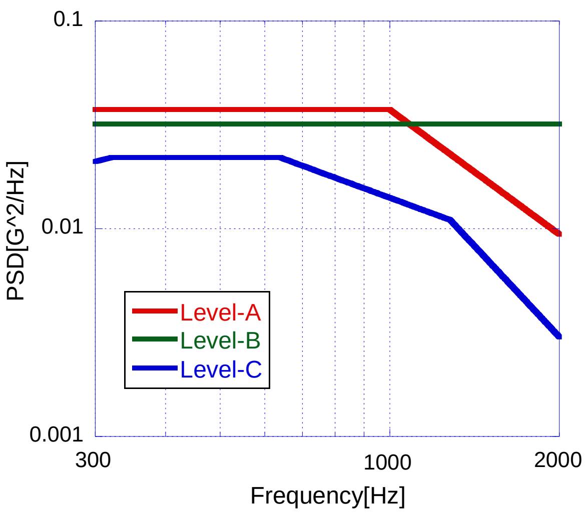

Fig. 14. Comparison of the AT test levels of various rockets in the range of 300-2000Hz.

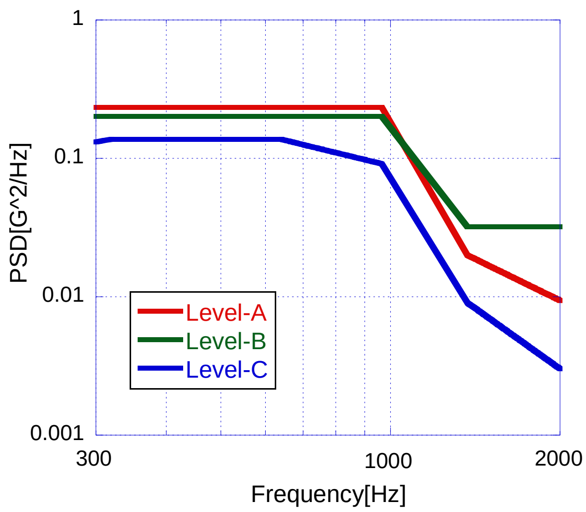

Fig. 15. Unit QT level (300-2000Hz)

We multiply the PSD shown in Fig. 14 by the square of the amplification factor shown in Fig.13. The result is shown as the unit QT level in Fig.15. It should be noted that the unit QT level shown in Fig.15 is the only minimum level for each test article to pass, not taking into account any margin. If a system developer, buyer of the product, wants to set margin, they have to choose the test level by themselves based on the specifics of their satellites.

4. Conclusion

NETS project for establishing environment test standard for micro/nano satellites started at KIT in 2011. In the present study, we deal with basic research for defining the qualification test (QT) level for COTS units in the framework of the NETS project.

We aimed to provide the minimum guarantee that a given unit sold as "a satellite unit" has a certain level of tolerance against space environment. The unit QT in the standard does not include proper margin against the maximum predicted environment stress, which depends on a satellite.

In order to determine unit QT level a series of vibration test were conducted and the input had not flat power spectrum comes from SMC up to 2000Hz. The 50cm class dummy satellite were tested for this purpose which is previously used for remote sensing in Japan.

In total, 46 points were measured within the satellite and 15 cases were studied in terms of excitation direction and accelerometer axis.

We noticed that there are two vibration modes and we call "whole satellite mode" and "local vibration mode". In this paper the test results and analyzing for local vibration mode were discussed. In whole vibration mode peaks at low frequencies were less than 300Hz. We found that those peaks are originated from the resonance of entire satellite structures to the vibration. In local vibration mode the peaks at frequencies higher than 300Hz are originated from the resonance of satellite internal structure. Internal units are exposed to those modes inside a satellite.

In this paper we proposed high and low limit of amplification factor and interval of resonance frequencies for local vibration mode. Finally, the unit QT random vibration test level was proposed for the frequency over 300Hz.

In the future, structure analysis will be done using finite element analysis (FEA) software tools to extrapolate the findings in the present paper to structures other than “yojo-han” structure studied in this paper.

Acknowledgments

The authors are grateful for the encouragement and support provided by Prof. Kuniaki Shiraki, Kyushu Institute of Technology and the members of NETS committee for their valuable comments.

References

1) Mengu Cho, Koichi Date, Shigekatsu Horii, Shoichi Obata: Introduction of Nanosatellite Environment Test Standardization (NETS) project, Background and Objectives. Joint-Conference on Space Technology and Science, December, 2011.

2) Kenta Tomida, Amgalanbat Batsuren,Toru Hatamura, Hirokazu Masui, Mengu Cho: Basic research on Vibration Test Level for Nanosatellite Components. 29^{th} International Symposium on Space Technology and Science, June, 2013.

3) George W.Snedecor, William G.Cochran: Statistical methods,1989, pp.31.